2012 American Control Conference
Fairmont Queen Elizabeth, Montréal, Canada
June 27-June 29, 2012

Investigating Controller Performance in Hybrid SOFC Systems with Unknown Nonlinearities

Tuhin Das and William Nowak

Abstract— **Solid oxide fuel cells (SOFCs) offer many benefits over various other fuel cells as a result of their high operating temperatures. Our prior work has addressed the conflicting goals of preventing fuel starvation and improving load-following in SOFCs through a combination of current regulation and hybridization with an ultra-capacitor. The associated controllers are largely model independent, excepting certain generalized assumptions that were made about the unknown and nonlinear dynamics of the SOFC's fuel supply system (FSS). In this paper we formulate a generalized structure of the control problem and controller from our earlier work, and relax the conditions imposed on the FSS. Thereafter, we analytically determine conditions of instability. We obtain inequality conditions that impose restrictions on the controller gains and the unknown nonlinearity. The conditions are helpful in predicting the limits of performance of the controller. The results are verified through simulations and through hardware-in-the-loop tests.**

I. INTRODUCTION

Solid oxide fuel cells (SOFCs) are energy conversion devices that operate by utilizing the electrochemical combination of hydrogen fuel and oxygen to produce water and electrical current. Due to their high operating temperatures $(800-1000°C)$, SOFC's are tolerant to fuel impurities, lend themselves well to bottoming cycle applications, capable of internal reforming and they do not require precious metal catalysts, [1]. Although SOFC's provide advantages, they are susceptible to fuel starvation. This transient phenomenon is detrimental to cell operation and integrity as it can cause voltage drop and anode oxidation. Fuel starvation is indicated by a performance variable known as fuel utilization, U. A 100% fuel utilization indicates fuel starvation. In order to balance electrical efficiency and safe operation, target U typically range between 70% and 90% [2], [3], [4].

In our prior work, we have developed a current regulation approach to control the transient response of U, [5]. Through this approach, the adverse effect of transient delays introduced by the fuel supply system (FSS) on U is minimized. The FSS represents a fuel pump and/or a valve along with a controller. The FSS supplies a fuel flow in response to a demanded fuel flow but introduces a transient delay. The corresponding regulated current causes a mismatch between the demanded and delivered power. To compensate for this mismatch, the SOFC system is hybridized with an ultra-capacitor. Thereafter robust control strategies are designed to stabilize the hybrid system in the presence of parameter uncertainties, [5], [6]. The objective of this paper is to investigate controller performance in the presence of unknown and nonlinear dynamics of the FSS.

First, the hybrid system is represented as a cascaded connection between the FSS dynamic and the SOC (State-of-charge) dynamic of the ultra-capacitor. A generalized cascaded system formulation is derived. Based on this formulation, a nominal control law is proposed in the absence of parameter uncertainties. Next, the closed-loop system is expressed as a Lur'e system [7], which allows the application of absolute stability concepts to investigate controller performance in the presence of unknown nonlinearity of the FSS. However simulations show that the condition for stability derived using this approach is conservative. By coordinate transformation, we express the closed-loop dynamics as a nonlinear mass-spring-damper system and use a storage function to derive a less conservative condition for stability. Next, in the presence of parameter uncertainties, an integral action is incorporated into the nominal controller for robustness. The integral action takes the form of an adaptive controller. For the resulting higher order closed-loop system, linearization is used to detect instability around the equilibrium point. The analysis yields inequality conditions that relate the controller gains and the local behavior of the nonlinear FSS. The results are verified through simulations as well as hardware-in-the-loop experiments.

II. BACKGROUND

A. STEAM REFORMING TUBULAR SOFC SYSTEM

A schematic of the system considered is included in Fig. 1 [8]. Methane fuel $\dot{N}_f$ enters the reformer where steam reacts with the fuel in the presence of a catalyst to produce hydrogen-rich gas. This reformed fuel, $\dot{N}_{in}$, then travels to the anode of the fuel cell stack. The stack has a tubular geometry such that the anode and cathode are arranged in concentric tubes. As current is drawn, electrochemical reactions occur in the stack causing steam-rich gas to flow out of the anode. A part of this exhaust flow $\dot{N}_o$ enters the combustor while a known amount, k, is recirculated back to the steam reformer. This recirculation sustains the endothermic reactions occurring in the reformer. While the combustion process burns excess fuel leftover from the electrochemical reactions in the stack, it also preheats $\dot{N}_{air}$ amount of air before it enters the cathode. The exhaust from the combustor finally circulates back to the steam reformer, further contributing heat to the reforming reactions [8].

Quantifying the operating conditions of the fuel cell system is typically done using the performance variable

This work was supported by the NSF under grant #1030744.

T. Das is an Assistant Professor at the University of Central Florida and W. Nowak was a graduate student of Mechanical Engineering at Rochester Institute of Technology, tdas@ucf.edu

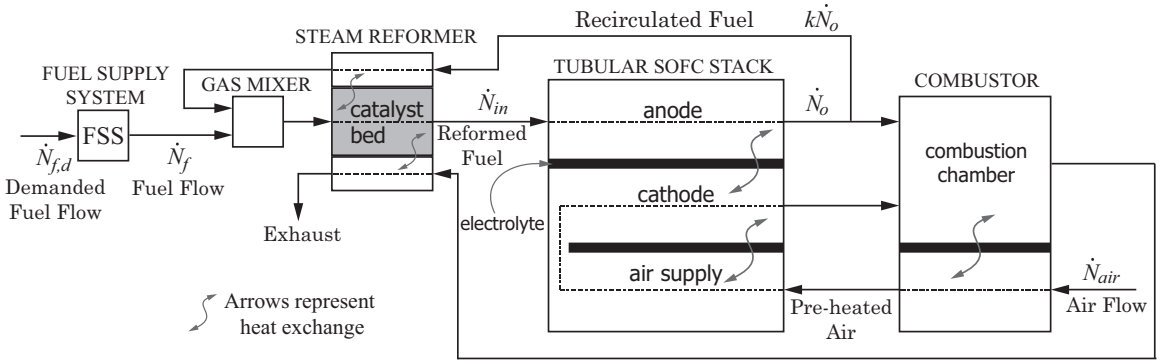

Fig. 1. Schematic diagram of steam reforming SOFC system

U. Fuel utilization, U, is defined as the ratio of hydrogen consumption to the net available hydrogen in the anode [2]. Considering the steady state expression for fuel utilization results in the following form [5]:

$$U = \frac{1-k}{(4nF\dot{N}_f/i_{fc}\mathcal{N}_{cell}) - k} \tag{1}$$

Eq. (1) is rearranged such that a demanded fuel flow $\dot{N}_{f,d}$ can be calculated given a demanded current $i_{fc,d}$ and a target U_{ss},

$$\dot{N}_{f,d} = \frac{i_{fc,d}\mathcal{N}_{cell}}{4nFU_{ss}}[1-(1-U_{ss})k] \quad \Rightarrow \quad \dot{N}_{f,d} = \sigma i_{fc,d} \tag{2}$$

where $\sigma = \mathcal{N}_{cell}[1-(1-U_{ss})k]/4nFU_{ss}$. Eq. (1) can be manipulated to compensate for delays along the fuel supply path by regulating current drawn from the system based on actual fuel flow,

$$i_{fc} = \frac{4nFU_{ss}\dot{N}_f}{\mathcal{N}_{cell}}\frac{1}{[1-(1-U_{ss})k} \quad \Rightarrow \quad i_{fc} = \sigma^{-1}\dot{N}_f \tag{3}$$

Since this strategy limits current based on fuel path delays, a hybridization technique can be implemented to compensate for the regulated current. It is also noted that the unknown dynamics of the FSS is represented by

$$\frac{d\dot{N}_f}{dt} = g(\dot{N}_f, \dot{N}_{f,d}) \tag{4}$$

B. HYBRID SYSTEM

For this hybrid system, an ultra-capacitor was used to compensate for the regulated fuel cell current. The hybrid system schematic is shown in Fig. 2. Both the fuel cell system and ultra-capacitor are connected to the electrical bus through DC/DC converters C_1 and C_2. C_1, connected to the fuel cell, is a unidirectional DC/DC converter which holds bus voltage V_L to 24V. C_2 is a bidirectional DC/DC converter which controls the ultra-capacitor current i_{uc}. The efficiencies of the converters, represented as η_1 and η_2, vary with operating conditions and are treated as unknown but bounded. It is also assumed that measurements of the fuel cell voltage V_{fc}, ultra-capacitor voltage V_{uc}, load current i_L and actual fuel flow $\dot{N}_f$ are available. From the system schematic, the instantaneous power balance is expressed as:

$$V_L i_L = \eta_1 V_{fc} i_{fc} + \eta_2 V_{uc} i_{uc} \tag{5}$$

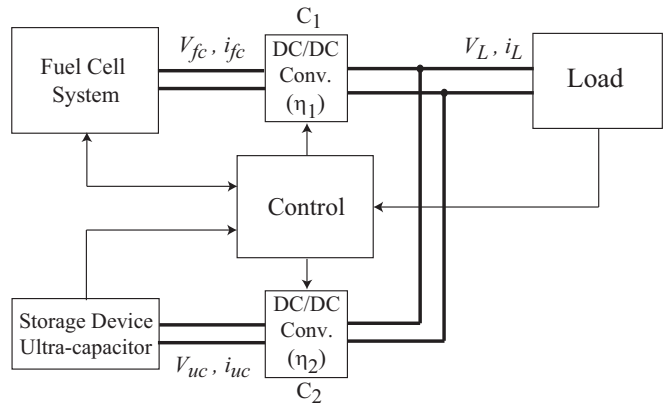

Fig. 2. Hybrid fuel cell system [5]

III. CASCADED SYSTEM

A. SOFC/UC AS A CASCADED SYSTEM

It is necessary to maintain the ultra-capacitor's SOC at a target value to avoid over-charging and over-discharging. Therefore, the development of the system state equations begins by considering error between the ultra-capacitor's SOC and the target SOC. This can be represented as

$$E_s = S - S_t, \quad S = \frac{V_{uc}}{V_{max}} \tag{6}$$

where S is the ultra-capacitor SOC, S_t is the target SOC, V_{uc} is the ultra-capacitor voltage and V_{max} is the maximum ultra-capacitor voltage. The dynamical equation of the ultra-capacitor and Eq. (6) then yield

$$\dot{V}_{uc} = -\frac{i_{uc}}{C} \quad \Rightarrow \quad \dot{E}_s = -\frac{i_{uc}}{CV_{max}} \tag{7}$$

From this relationship of $\dot{E}_s$, the hybrid system power balance expression in Eq. (5) can be used to represent the error in the ultra-capacitor's SOC as the following:

$$\dot{E}_s = -\left(\frac{1}{CV_{max}}\right)\left[\left(\frac{V_L i_L}{\eta_2 V_{uc}}\right) - \left(\frac{\eta_1 V_{fc}}{\eta_2 V_{uc}}\right) i_{fc}\right] \tag{8}$$

However, i_{fc} is not the control input. The control input is $i_{fc,d}$ and, denoting that $E_{fc} = i_{fc} - i_{fc,d}$, we have

$$\dot{E}_s = -\left(\frac{1}{CV_{max}}\right)\left[\left(\frac{V_L i_L}{\eta_2 V_{uc}}\right) - \left(\frac{\eta_1 V_{fc}}{\eta_2 V_{uc}}\right)(E_{fc} + i_{fc,d})\right] \tag{9}$$

Thus from Eqs. (2), (3), (4) and (8), we have the following cascaded system:

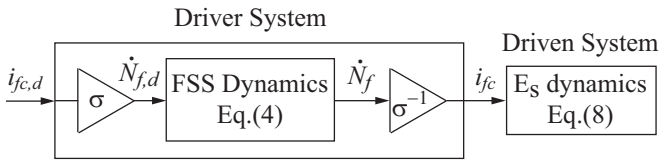

Fig. 3. SOFC/UC hybrid as a cascaded system

B. GENERALIZED CASCADED SYSTEM

The cascaded system consists of the unknown FSS dynamics acting as a driver system and the ultra-capacitor SOC state equation acting as the driven system. From the arrangement shown in Fig. 3 and from Eq. (9), a generalized system is illustrated in Fig. 4, where

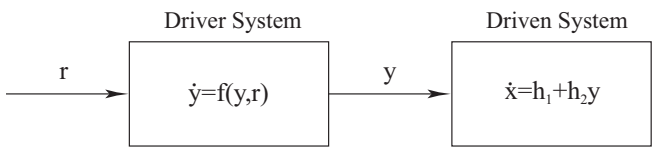

Fig. 4. Cascaded system in the general form

$$y \equiv i_{fc}, \quad r \equiv i_{fc,d}, \quad x \equiv E_s, \quad \dot{x} = h_1 + h_2 y \tag{10}$$

and

$$h_1 = -\frac{1}{\eta_2}\left(\frac{V_L i_L}{C V_{max} V_{uc}}\right), \quad h_2 = \frac{\eta_1}{\eta_2}\left(\frac{V_{fc}}{C V_{max} V_{uc}}\right) \tag{11}$$

Note that $f(y,r)$ is the unknown nonlinearity representing the fuel supply system (FSS). The overall state-space model of the system is therefore given by

$$\dot{y} = f(y,r), \quad \dot{x} = h_1 + h_2 y \tag{12}$$

IV. ANALYSIS WITHOUT UNCERTAINTIES

A. LUR'E SYSTEM FORMULATION

In this section, we show that the system dynamics given by Eq. (12), together with a feedback control law, can be expressed as a Lur'e system [7] where the FSS dynamics being treated as the unknown nonlinearity. Here, h_1 and h_2 are treated as known and constant and driver system input r and driven system input y from Fig. 4 are related by the error equation

$$y = e + r \tag{13}$$

Driver system input r is designed as

$$r = \frac{h_1}{h_2} - kx \tag{14}$$

From Eq. (10), (13) and (14),

$$\dot{x} = -h_2 k x + h_2 e \tag{15}$$

From Eqs. (12) and (13),

$$\dot{y} = f(y,r) \;\rightarrow\; \dot{e} + \dot{r} = f(e+r,r) \tag{16}$$

From Eq. (15) and (16), we have,

$$\dot{e} = f(e+r,r) + k\dot{x} = f(e+r,r) + kh_2 e - h_2 k^2 x \tag{17}$$

This results in the closed loop system state equations below:

$$\begin{aligned} \dot{x} &= -h_2 k x + h_2 e \\ \dot{e} &= f(e+r,r) + kh_2 e - h_2 k^2 x \end{aligned} \tag{18}$$

where $f(e+r,r)$ represents the unknown nonlinearity, consider the following coordinate transform:

$$z = e - kx \tag{19}$$

then,

$$\begin{aligned} \dot{z} &= f(e+r,r) \\ \dot{e} &= f(e+r,r) + kh_2 z \end{aligned} \tag{20}$$

Given this closed loop state-space model in Eq. (20), the remaining work will consider the case where unknown nonlinearity $f(e+r,r) \equiv f(e)$ with $f(e) = 0$ when $e = 0$. Physically, the implication of this assumption is that the general FSS dynamics $\dot{e} = f(e+r,r)$ induces no steady state error. Letting $u = -\psi$ where the nonlinearity $\psi = -f(e)$, Eq. (20) can be given as

$$\begin{bmatrix} \dot{z} \\ \dot{e} \end{bmatrix} = \begin{bmatrix} 0 & 0 \\ kh_2 & 0 \end{bmatrix} \begin{bmatrix} z \\ e \end{bmatrix} + \begin{bmatrix} 1 \\ 1 \end{bmatrix} u \tag{21}$$

Considering e to be the output variable, the resulting transfer function is given as

$$\frac{e(s)}{u(s)} = G(s) = \frac{s + kh_2}{s^2} \tag{22}$$

Which leads to the following Lur'e system formulation:

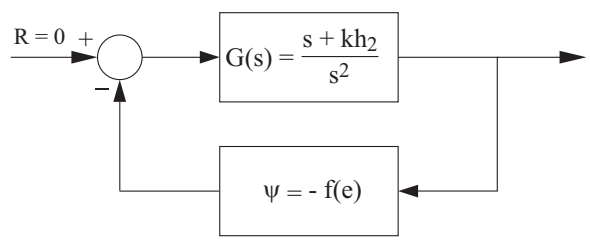

Fig. 5. Generalized SOFC/UC hybrid in Lur'e form

B. ABSOLUTE STABILITY ANALYSIS

The *Circle Criterion* is first used to obtain a sector condition on the nonlinearity that will ensure stability of the Lur'e system in Fig. 5. This sector condition is given as $\psi \in [K_1, \infty]$, where $K_1 > 0$ and K_1 must be such that $\hat{G}(s) = G(s)[I + K_1 G(s)]^{-1}$ is strictly positive real. From *Definition 6.4* [7] we can show that this is the case if $K_1 > \epsilon > 0$ and $K_1 > \frac{kh_2}{2}$. This places a constraint between the sector condition K_1 on the unknown nonlinearity and feedback gain k and h_2 defined in Eq. (11). The following simulations will be used to test sample general FSS behaviors $f(e)$ that meet the sector condition $[K_1, \infty]$ and also behaviors that violate this condition.

The following simulations show that the sector condition imposed by the Circle Criterion is conservative. The sector condition to be met is shown by the shaded area in Figs. 6

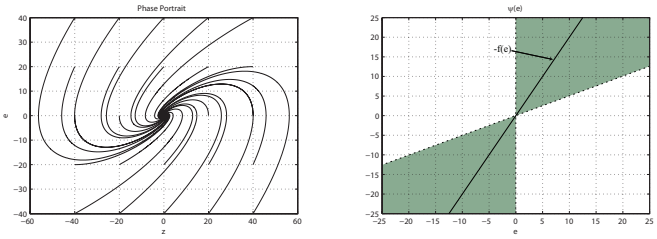

Fig. 6. Absolute stability simulation case 1: $-f(e) \in [K_1, \infty]$

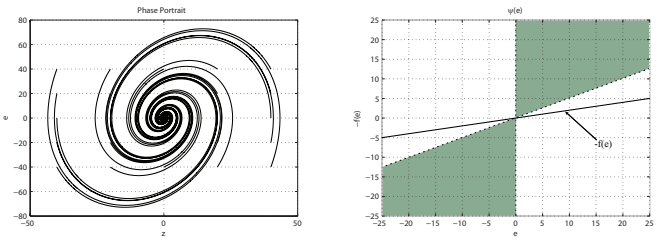

Fig. 7. Absolute stability case 2: $-f(e) \notin [K_1, \infty]$

and 7 For the first case, the sector condition was met by simulating a simple function $\psi = -f(e) = ae$ for the general fuel supply system dynamic equation. For the second case, the condition was not met. The corresponding phase portraits are also plotted. From these simulations, it can be concluded that absolute stability can be used to ensure stability of this generalized system for a class of nonlinearities. However, these results prove to be conservative. The following section will explore a Lyapunov based stability approach for the general cascaded system.

C. LYAPUNOV STABILITY ANALYSIS

Using Eq. (20), a single second order expression is derived such that,

$$\ddot{e} + \frac{df}{de}\dot{e} + kh_2 f(e) = 0 \tag{23}$$

where $\dot{e}$ and e are considered the states. The Lyapunov function candidate is chosen as the energy storage function

$$V = \frac{1}{2}\dot{e}^2 + \int_0^e kh_2 f(e)de. \tag{24}$$

Taking the derivative of Eq. (24) along the state trajectories and using Eq. (23) results in the following:

$$\dot{V} = \dot{e}(-\tfrac{df}{de}\dot{e} - kh_2 f(e)) + kh_2 f(e)\dot{e} = -\tfrac{df}{de}\dot{e}^2 \;\leq\; 0 \tag{25}$$

Since $\dot{V}$ can only be concluded to be negative semidefinite, the *invariance principle* is used [7]. Considering Eq. (25),

$$\dot{V} = 0 \;\Rightarrow\; \dot{e} = 0 \;\Rightarrow\; \ddot{e} = 0 \tag{26}$$

From Eq. (23), $f(e) = 0 \;\Rightarrow\; e = 0$ Therefore, it can be concluded that $e = \dot{e} = 0$ is asymptotically stable provided that

$$\frac{df}{de} \;>\; 0 \;\forall\, e \tag{27}$$

This condition is independent of the system characteristics k and h_2. The following simulations will verify these findings.

Simulations were performed with $kh_2 = 1$, and with an array of initial conditions. Fig. 8 provides results when

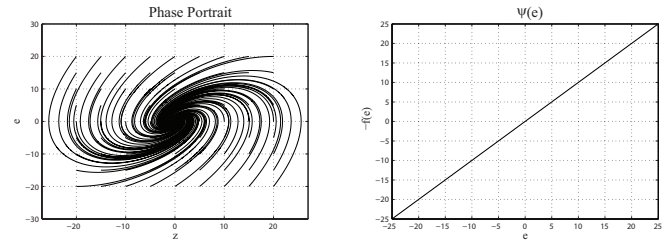

Fig. 8. Positive df/de

$df/de = 1$, hence meeting the stability criteria from Eq.(27). In this case, all state trajectories converge to the origin as expected. In Fig. 9, as FSS behavior of $f(e) =$

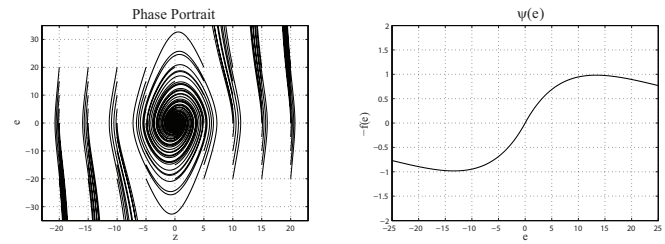

Fig. 9. Positive/negative df/de

$20\text{sgn}(e)\,[\exp(-0.7|e|) - \exp(-0.8|e|)]$. From the results, it is clear that the equilibrium now only has local stability due to the negative gradient of $f(e)$. It can be seen that the condition in Eq.(27) is less conservative compared to the sector condition obtained in section IV-B. Next we continue to investigate the effects of the nonlinear FSS behavior in the presence of uncertainties in h_1 and h_2.

V. PERFORMANCE OF ROBUST CONTROLLER

We now treat h_1 and h_2 given in Eq. (11) as unknown parameters and design an adaptive controller. The controller results in an integral control for the closed loop system.

A. GENERALIZED ADAPTIVE CONTROL STRATEGY

This analysis will begin by considering the generalized hybrid system equations presented in Section IV-A, Eq. (12), (13) and (16) yield the following system equations:

$$\begin{aligned} \dot{x} &= h_1 + h_2(e + r) \\ \dot{e} &= -f(e + r, r) - \dot{r} \end{aligned} \tag{28}$$

The fuel supply system behavior will be assumed to follow the general behavior $f(e + r, r) = f(e)$ and h_1 and h_2 given in Eq. (11) are slowly varying, unknown and bounded quantities. Control input r shown in the following equation is designed to cancel out the effects of h_1 in Eq. (28) and stabilize error in the ultra-capacitor SOC $E_s = x$.

$$r = -\frac{\hat{h}_1}{\hat{h}_2} - kx \tag{29}$$

Since h_1 and h_2 are unknown, estimates $\hat{h}_1$ and $\hat{h}_2$ of h_1 and h_2 respectively are used in the control law. Implementing the control design from Eq. (29) on the generalized system equation from (28), the closed loop system equations are presented as in the following where parameter error $e_{12} = \frac{h_1}{h_2} - \frac{\hat{h}_1}{\hat{h}_2}$ and $\mathcal{E} = \frac{d}{dt}\left(\frac{\hat{h}_1}{\hat{h}_2}\right)$,

$$\begin{aligned} \dot{x} &= h_2 e_{12} + h_2(e - kx) \\ \dot{e} &= -f(e) + kh_2 e_{12} + kh_2(e - kx) + \mathcal{E} \end{aligned} \tag{30}$$

Using the adaptation law

$$\dot{e}_{12} = -\gamma x \tag{31}$$

and the following transform

$$v = \gamma x - \dot{e} - f(e) \tag{32}$$

results in

$$\begin{aligned} &\ddot{e} + \tfrac{df}{de}\dot{e} + kh_2 f(e) = -\tfrac{\gamma}{k} v \\ &\dot{v} = kh_2 f(e) \end{aligned} \tag{33}$$

The following section will analyze the stability of this closed-loop system.

B. STABILITY ANALYSIS OF ADAPTIVE CONTROL

Considering the generalized closed loop system with adaptive control from Eq. (33), the state space representation is formulated where $x_1 = e$, $x_2 = \dot{e}$ and $x_3 = v$. The state space form is given as,

$$\begin{bmatrix} \dot{x_1} \\ \dot{x_2} \\ \dot{x_3} \end{bmatrix} = \begin{bmatrix} x_2 \\ -kh_2 f(x_1) - \frac{df(x_1)}{dx_1} x_2 - \frac{\gamma}{k} x_3 \\ kh_2 f(x_1) \end{bmatrix} \tag{34}$$

In order to analytically examine limitations of the adaptive controller with unknown fuel supply system behavior, this system is linearized about the origin. With a linear approximation of the FSS behavior $f(x_1) = ax_1$. The linear system matrix A_{lin} of the closed loop system at $x_1 = x_2 = x_3 = 0$ is obtained as:

$$A_{lin} = \begin{bmatrix} 0 & 1 & 0 \\ -kh_2 a & -a & -\frac{\gamma}{k} \\ kh_2 a & 0 & 0 \end{bmatrix}, \tag{35}$$

and the characteristic equation is

$$0 = s^3 + as^2 + kh_2 as + h_2 a\gamma. \tag{36}$$

Using *Routh's Stability Criterion*, [9], it can be shown that

$$ka > \gamma \tag{37}$$

is a necessary and sufficient condition for stability of the closed loop system for small perturbations about the equilibrium.

VI. RESULTS

A. HYBRID SYSTEM SIMULATIONS

To confirm the stability criterion of Eq.(37), simulation results with $V_L = 24V$, $U_{ss} = 80\%$, target SOC $S_t = 0.8$, ultra-capacitor $C = 250F$ and $V_{max} = 16.2V$. The parameter estimates $\hat{\eta}_1$ and $\hat{\eta}_2$ are initialized at 0.92. The FSS is modeled as $N_f(s)/N_{f,d}(s) = 1/(2s+1)$, hence $a = 0.5$, but is treated as unknown to the controller. Also a value of $k = 70$ was chosen so that the equilibrium is stable for $\gamma < 35$ and unstable otherwise.

Fig. 10 shows the system response to a constant input of $i_L = 10A$. This simulation was run with $\gamma = 46$ when $t < 450\,\text{s}$ and $\gamma_1 = 23$ when $t \geq 450\,\text{s}$. The two values of γ were sufficiently separated from the threshold with the understanding that the parameters assumed constant are actually time varying and hence Eq.(37) provides an estimate. The adaptation is off initially and switched on at $t = 250\text{s}$.

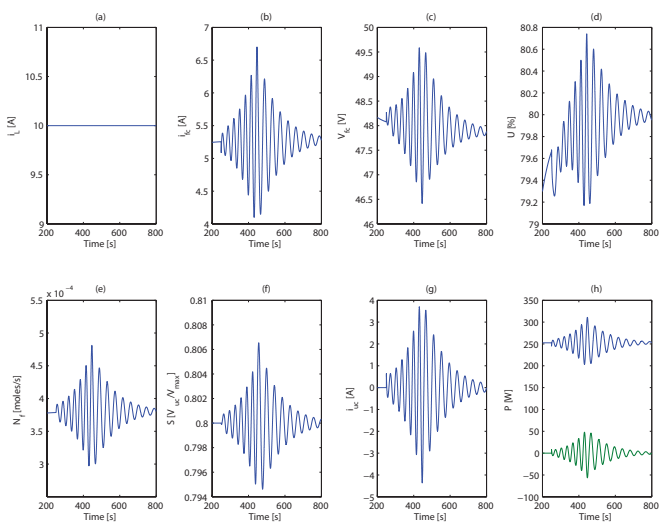

Fig. 10. Simulation with adaptive control and $i_L = 10A$

In this simulation, it is clear that the equilibrium is unstable when γ is set above the calculated threshold. Expectedly, the equilibrium stabilizes for $t > 450$ s when γ is switched to a value below the threshold.

B. EXPERIMENTAL RESULTS

A hardware-in-the-loop (HIL) setup is used for experimental validation. The system is shown in Fig. 11. The SOFC system described in section II-A is modeled and emulated using a dSPACE DS1103PPC controller board and a SGA series Sorensen DC programmable power supply. The mathematical model of the SOFC is described in [8]. The emulated fuel cell is connected to the load using a SD-1000L-24 unidirectional DC/DC converter from Mean Well. A $16.2V$ series BMOD0250-E016 ultra-capacitor from Maxwell Technologies with a $250F$ capacitance and $4.1m\Omega$ resistance is connected in parallel to the fuel cell. It is interfaced using a DC5050F-SU bidirectional DC/DC converter from Zahn Electronics, Inc. A Sorensen $1.8kW$ SLH series

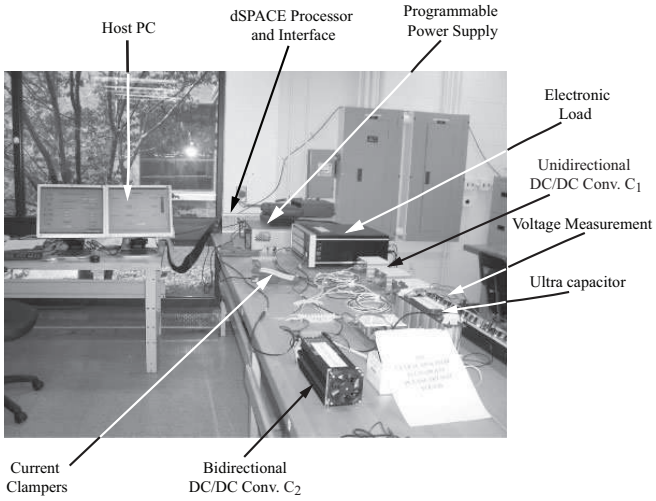

Fig. 11. Harware-in-the-loop (HIL) test stand

DC programmable electronic load is used for power draw. Further details pertaining to this system can be found in [5].

Experiments were conducted on the HIL setup with $V_L = 24V$, $U_{ss} = 80\%$, target SOC $S_t = 0.8$, ultra-capacitor $C = 250F$ and $V_{max} = 16.2V$. The parameter estimates $\hat{\eta}_1$ and $\hat{\eta}_2$ are both initialized at 0.92. The FSS is modeled as $\dot{N}_f(s)/\dot{N}_{f,d}(s) = 0.85/(2s+1)$ but is treated as unknown. Also, $k = 70$ for the HIL tests as well. In the plots, $t = 0\,\mathrm{s}$ is the start of parameter estimation and data capture. Fig. 12

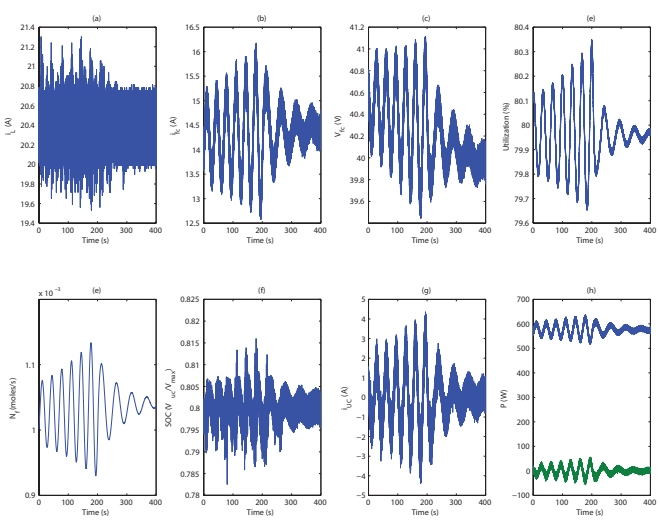

Fig. 12. HIL experiments with adaptive control and $i_L = 20A$

shows the simulation results for $\gamma = 50$ when $t < 200\,\mathrm{s}$ and $\gamma = 20$ when $t \geq 200\,\mathrm{s}$. The results indicate an unstable equilibrium for $t < 200\,\mathrm{s}$ which becomes stable when the stability criterion is satisfied, as expected. Although there is error induced in various stages of the process, the general result of Eq.(37) provides a relatively good approximation. Additionally, it has been shown that the stability result is applicable for various load demands.

VII. CONCLUSIONS

This paper investigated the performance of controllers designed for hybrid SOFC systems in our prior work [6], when the simplifying assumptions about the unknown dynamics of the FSS are lifted. Using a generalized cascaded system formulation and absolute stability concepts, classes of possible FSS behaviors were examined and their effects on system stability studied in the absence of uncertainties. An adaptive controller was used when the DC/DC converter efficiencies were considered uncertain. The controller was restructured in a generalized form. Through linearization, the criterion for instability was derived as an inequality condition. The condition is governed by local behavior of the FSS around the origin, feedback gain and parameter estimation gain. This result was verified using both simulations and experiments on an HIL test stand. The results supported the initial relationship, holding true at varying load demand levels. This relationship would be useful in future work for sizing gains, preventing instability and possible component damage.

REFERENCES

[1] J. Larminie and A. Dicks. *Fuel Cell Systems Explained*. John Wiley and Songs Ltd., 2003.

[2] A. Lazzaretto, A. Toffolo, and F. Zanon. Parameter setting for a tubular sofc simulation model. *Transactions of the ASME. Journal of Energy Resources Technology*, 126(1):40–6, 2004.

[3] K. Sedghisigarchi and A. Feliachi. Control of grid-connected fuel cell power plant for transient stability enhancement. *2002 IEEE Power Engineering Society Winter Meeting. Conference Proceedings (Cat. No.02CH37309)*, vol.1:383–8, 2002.

[4] S. Campanari. Thermodynamic model and parametric analysis of a tubular sofc module. *Journal of Power Sources*, 92(1-2):26–34, 2001.

[5] T. Allag and T. Das. Robust control of solid oxide fuel cell ultracapacitor hybrid systems. *IEEE Transactions on Control Systems Technology*, in press, 2011.

[6] T. Das and S. Snyder. Adaptive control of a solid oxide fuel cell ultra-capacitor hybrid system. *Proceedings of the American Control Conference, San Francisco, CA*, 2011.

[7] H. Khalil. *Nonlinear Systems*. Prentice-Hall, Inc., Upper Saddle River, NJ, 3 edition, 2002.

[8] T. Das, S. Narayanan, and R. Mukherjee. Steady-state and transient analysis of a steam-reformer based solid oxide fuel cell system. *Journal of Fuel Cell Science and Technology*, 7(1), 2010.

[9] K. Ogata. *Modern Control Engineering*. Prentice-Hall, Inc., Upper Saddle River, NJ, 4 edition, 2002.